Analysis of Long Time Series of Polar Motion

SEMINAR

Wei-Yung Chung
鍾霨詠

Introduction

- Free Euler motion

  Chandler wobble ： P=~~300~~ day

  P ≒ 433.7day

  input → Earth rotation → output

- Parameter examination : period P and Q-value

References

1. B. F. Chao, 1983. Autoregressive harmonic analysis of the Earth's polar motion using homogeneous international latitude service data. J. Geophys. Res., 88(B12), 299-10

2. M. Furuya and B. F. Chao., 1996. Estimation of period and *Q* of the Chandler wobble. Geophys. J. Int. 127, 693-702

3. H. Schuh, S. Nagel, and T. Seitz, 2001. Linear drift and periodic variations observed in long time series in polar motion., J. Geodesy, 74, 701

1

Data

- International Latitude Service (ILS)
  - 80-year-long (1900-1979)
  - Monthly

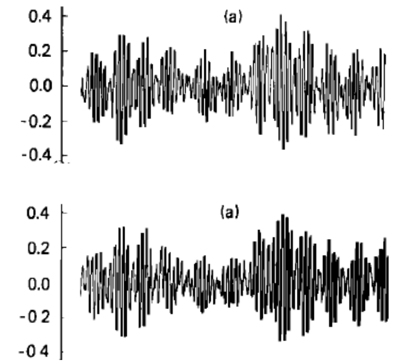

Method

Autoregressive harmonic analysis **[Chao and Gilbert, 1980]**

$$x(n) = \sum_{j=1}^{M} [A_j \exp(in\sigma_j) + A_j^* \exp(-in\sigma_j^*)] \qquad (1)$$

$$n = 1, 2, 3, \cdots, N$$

$$x(n) = \sum_{i=1}^{2M} S_i x(n-i) \qquad n = 2M+1, \cdots, N \qquad (2)$$

$$Z^{2M} - S_1 Z^{2M-1} - S_2 Z^{2M-2} - \cdots - S_2$$

$$= \sum_{j=1}^{M} [Z - \exp(i\sigma_j)][Z - \exp(-i\sigma_j^*)] \qquad (3)$$

2Mth degree polynomial equation in complex variable Z

1

Hanning-windowed Fourier power spectrum

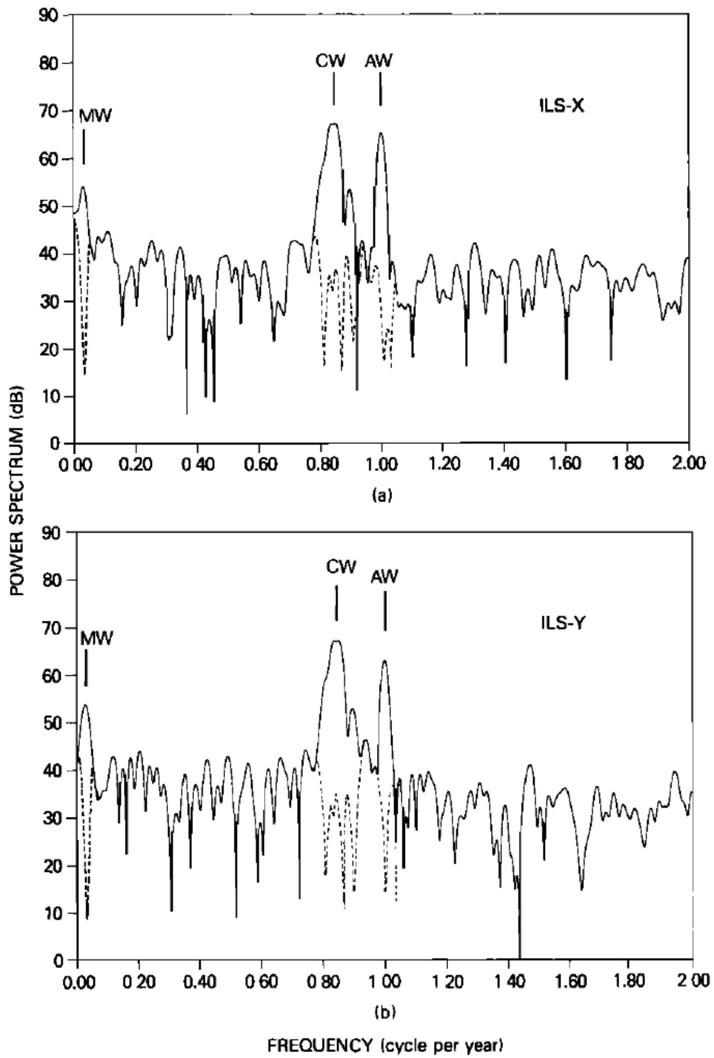

Markowitz wobble (MW)
annual wobble (AW)
Chandler wobble (CW)

ILS-X-CW

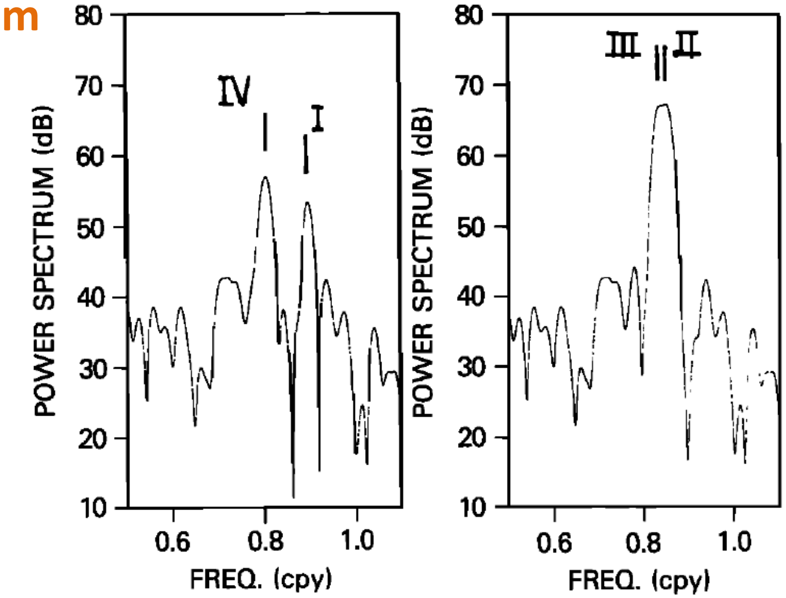

ILS-Y-CW

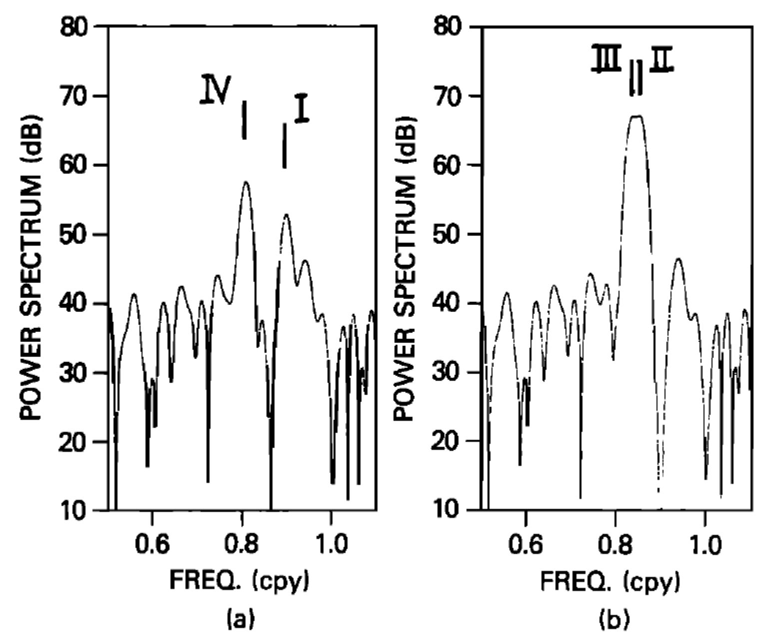

1

Markowitz Wobble

X component

Y component

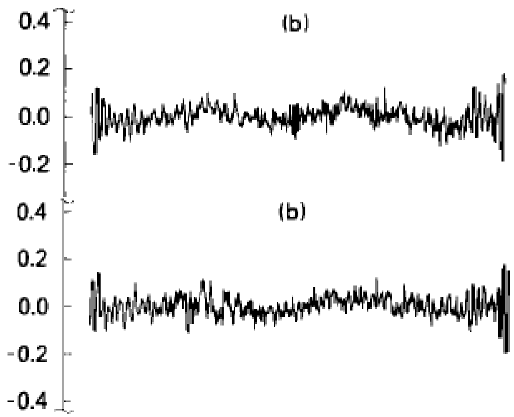

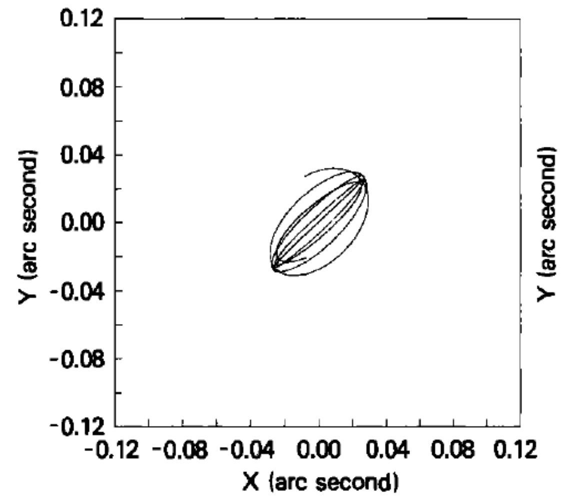

TABLE 1. AR Estimates for the Markowitz Wobble

	Period, years	Q	Amplitude (0.001 arc sec)	Phase, deg
ILS-X	29.6 ± 1.1	>15, < −11	24.6 ± 4.4	197 ± 10
ILS-Y	31.7 ± 0.9	>25, < −12	23.0 ± 3.2	242 ± 8

It is marginally retrograde (ILS-YMW lags ILS-X-MW by 45 ± 18 °)

$1/Q = (1/Q_1 + 1/Q_2)/2$ Q=-88 for ILS-X , Q=-43 for ISL-Y

Q>0 amplitude decay , Q<0 amplitude grows

1

Annual Wobble

X component

Y component

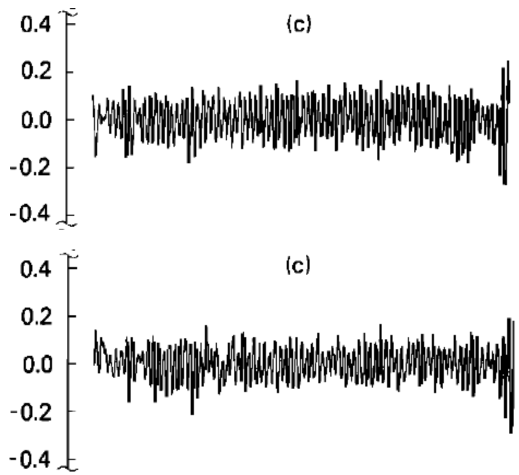

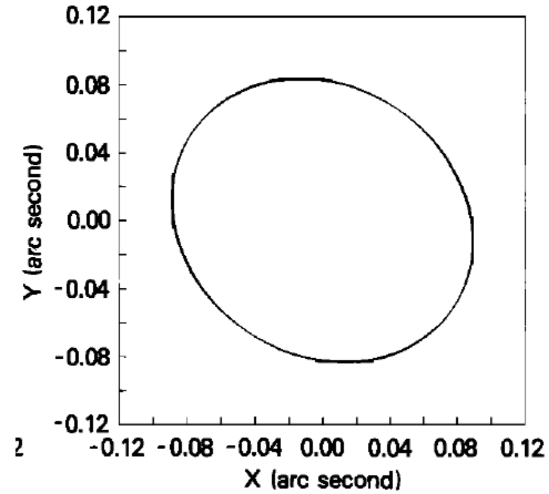

TABLE 2. AR Estimates for the Annual Wobble

	Period, days	Q	Amplitude (0.001 arc sec)	Phase, deg
ILS-X	365.20 ± .08	−930 ~ −3700	88.4 ± 2.5	108 ± 2
ILS-Y	365.10 ± .10	800 ~ 4600	84.0 ± 3.0	10 ± 2

ILS-X-AW leads ILS-Y-AW by 98 ± 4 °, giving an almost purely prograde motion

1

Chandler Wobble

TABLE 3*a*. AR Estimates for the Chandler Wobble From ILS-X

Component	Period, days	Q	Amplitude (0.001 arc sec)	Phase, deg
I	406.45 ± .29	> 500, < −1080	26.7 ± 2.4	216 ± 5
II	426.00 ± .08	711 ± 27%	119.9 ± 2.7	273 ± 1
III	437.46 ± .09	−189 ± 8%	57.3 ± 1.3	342 ± 1
IV	452.73 ± .27	180 ± 22%	68.6 ± 4.3	150 ± 4

TABLE 3*b*. AR Estimates for the Chandler Wobble From ILS-Y

Component	Period, days	Q	Amplitude (0.001 arc sec)	Phase deg
I	406.85 ± .42	−210 ~ −1930	17.0 ± 2.1	132 ± 7
II	426.15 ± .10	703 ± 34%	119.5 ± 3.4	185 ± 2
III	437.43 ± .11	−184 ± 10%	57.2 ± 1.6	253 ± 2
IV	452.39 ± .33	220 ~ 600	56.9 ± 4.5	54 ± 5

X component

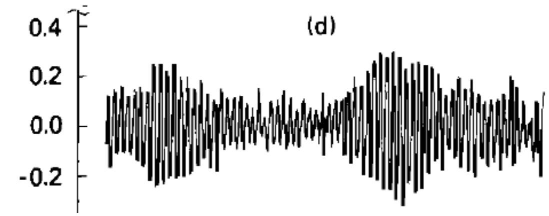

Y component

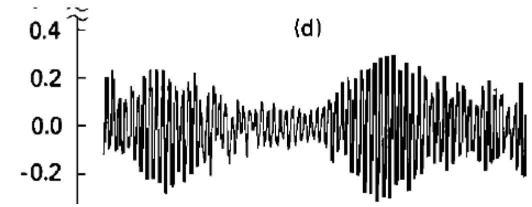

We considers the Chandler wobble as a single component with a fixed period and an amplitude modulated by a sequence of temporally and/or spatially random excitation

1

Chandler wobble motion

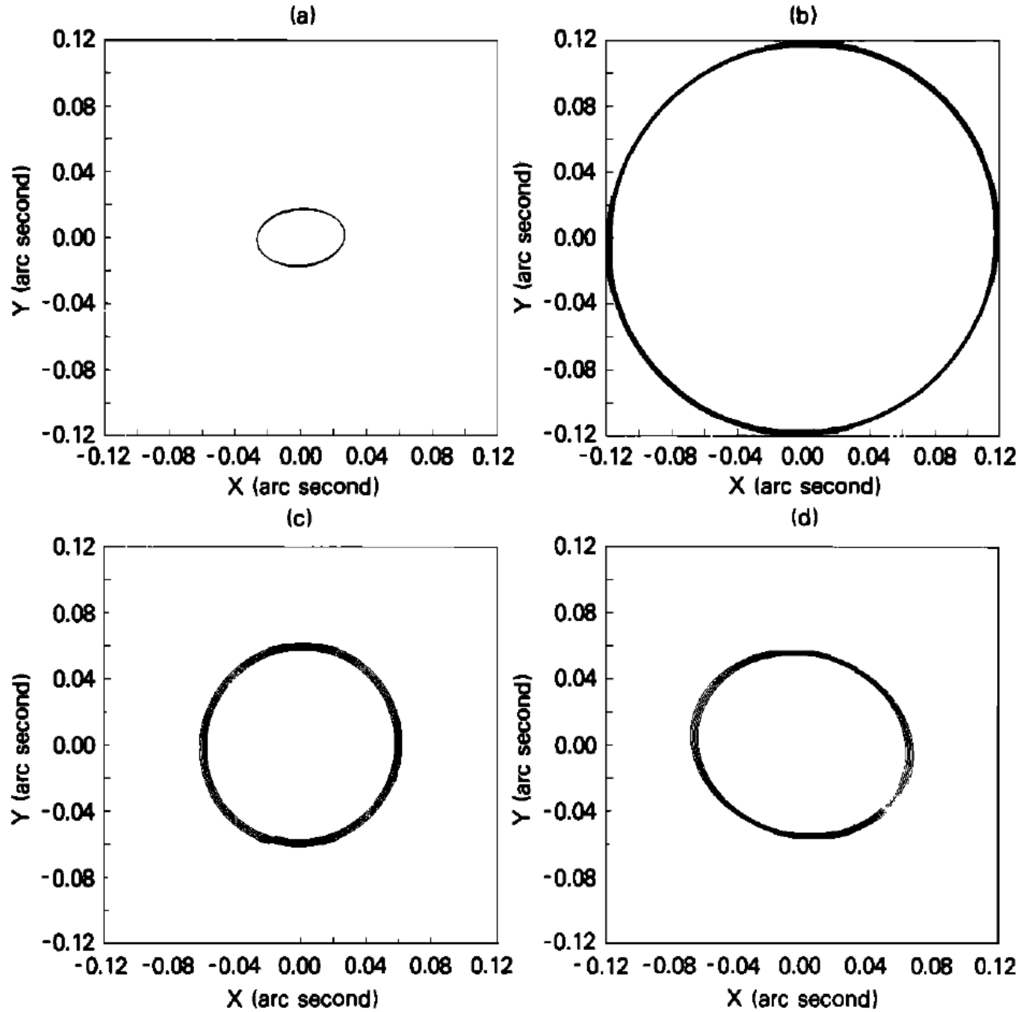

1

The time variations in the amplitude and phase of the polar wobbles

Complex demodulation

$$\Gamma_f(t) = \frac{1}{2L+1} \sum_{|t-u| \leq L} z(u) \exp(-i2\pi f u)$$

$$z(t) = (\text{ILS-X-AW}) + i(\text{ILS-Y-AW})$$

$$z(t) = (\text{ILS-X-CW}) + i(\text{ILS-Y-CW})$$

$\lvert\Gamma_f(t)\rvert$	running amplitude
$\arg(\Gamma_f(t))$	running phase

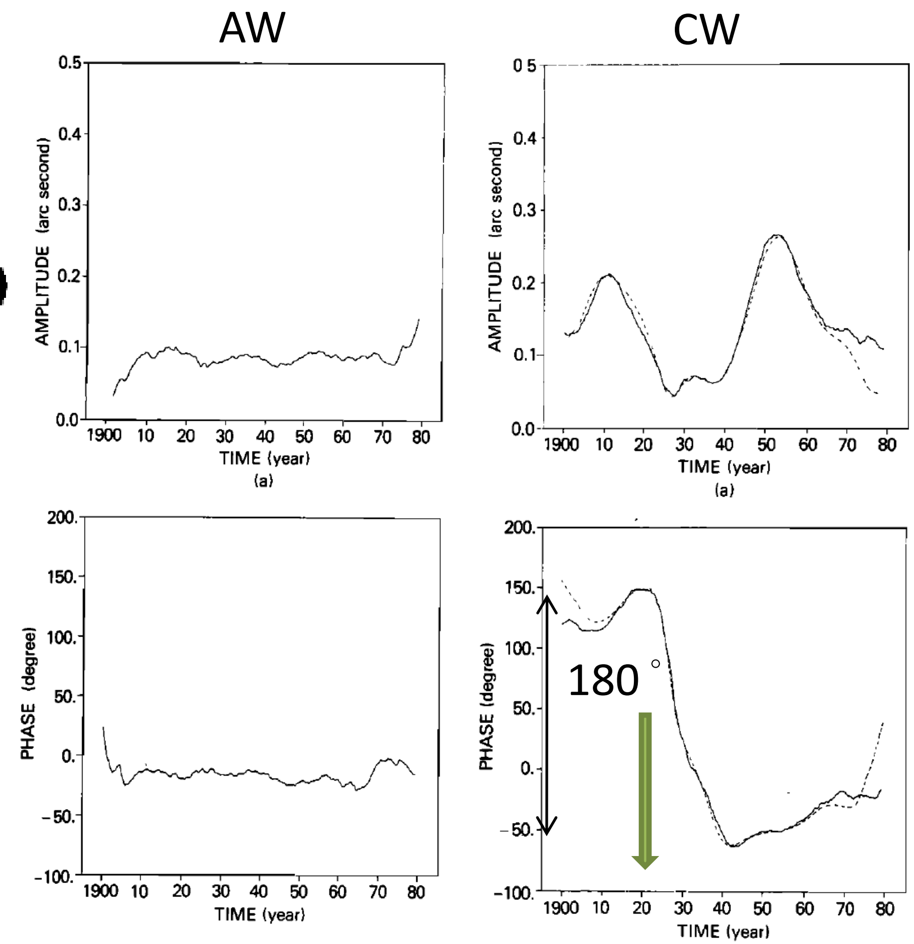

A "center Chandler period" of 432.00 days is shown as solid lines. Dashed lines is of the four component synthetic Chandler series.

1

Points

- Chandler wobble can be adequately modeled as a linear combination of four harmonic components
- The model "explains" the apparent phase reversal during 1920-1940
- the annual wobble is shown to be rather stationary over the year
- the Markowitz wobble is found to be marginally retrograde and appears to have a complicated behavior which cannot be resolve

2

Optimization criteria

$$\text{AAM} = (\text{wind term}) + \gamma\,(\text{pressure IB term}) + (1\text{-}\gamma)\,(\text{pressure term})$$

$$D(P,Q)\,m(t) = \chi(t) = \text{AAM}(\gamma,t) + \chi_{\mathbf{na}}(t)$$

- After removal of coherent seasonal and long-period signals, the non-AAM excitation is uncorrelated with the AAM

We allow γ *to* be complex-valued so that its (presumably small) imaginary part allows for any (east-west) phase differences among the terms in equation.

Data

- Space94
  - 10.8yr (1976~)
  - Kalman filter
  - Daily (Nyquist period ~10day)
- Atmospheric angular momentum (AAM)
  - Japan Meteorological Agency (JMA)
  - 1983 -1992 →daily, 10.8yr
  - Butterworth filter 10day
  - US Nation Meteorological Center (NMC) also prepared

2

Monte Carlo simulation

- I
  - seeks to minimize the non-AAM χ_{na} variance with respect to the variations in the three parameters *P, Q and y.*
    - Ia. chosen to contain four elementary Fourier bins, from 0.67 to 0.94 cycle per year (cpy)
    - Ib. uses 64 elementary bins from 0.49 to 6.11 cpy
    - Ic. uses 134 bins from -6.11 to 6.1 1 cpy
- II
  - seeks to maximize the cross-correlation between the excitation function and AAM with respect to the variations in the three parameters *P, Q and y.*

2

Monte Carlo simulation

- I
  - perform a non-linear, iterative search in the 3-D (P,Q,y) space for the minimum of the residual spectral power R of the non-AAM excitatior χ_{na}

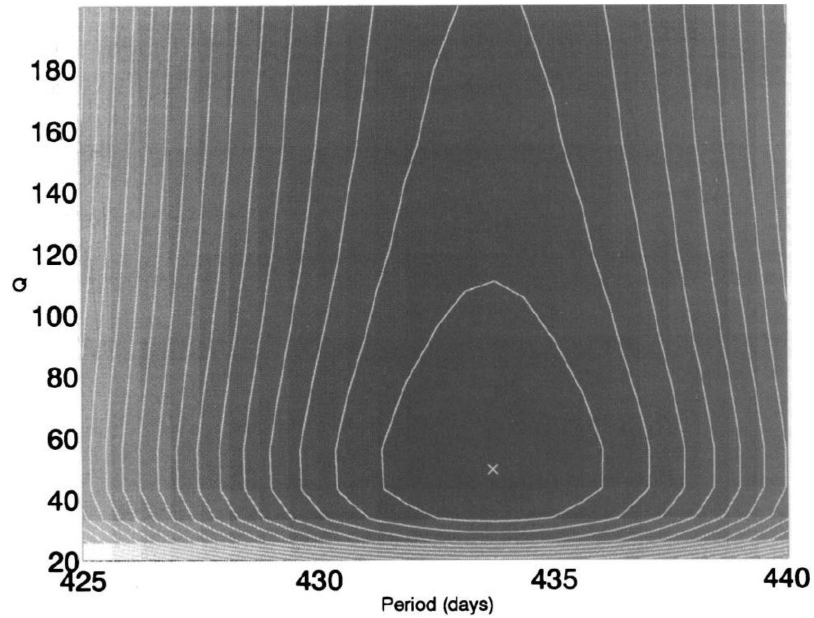

- II
  - a non-linear, iterative in the 3-D (P,Q,y) space for the maximum of the absolute value of the cross-correlation function between the ensuing AAM and the excitation function x, which invariably occurs as a prominent peak at zero time-shift

Results Ia.

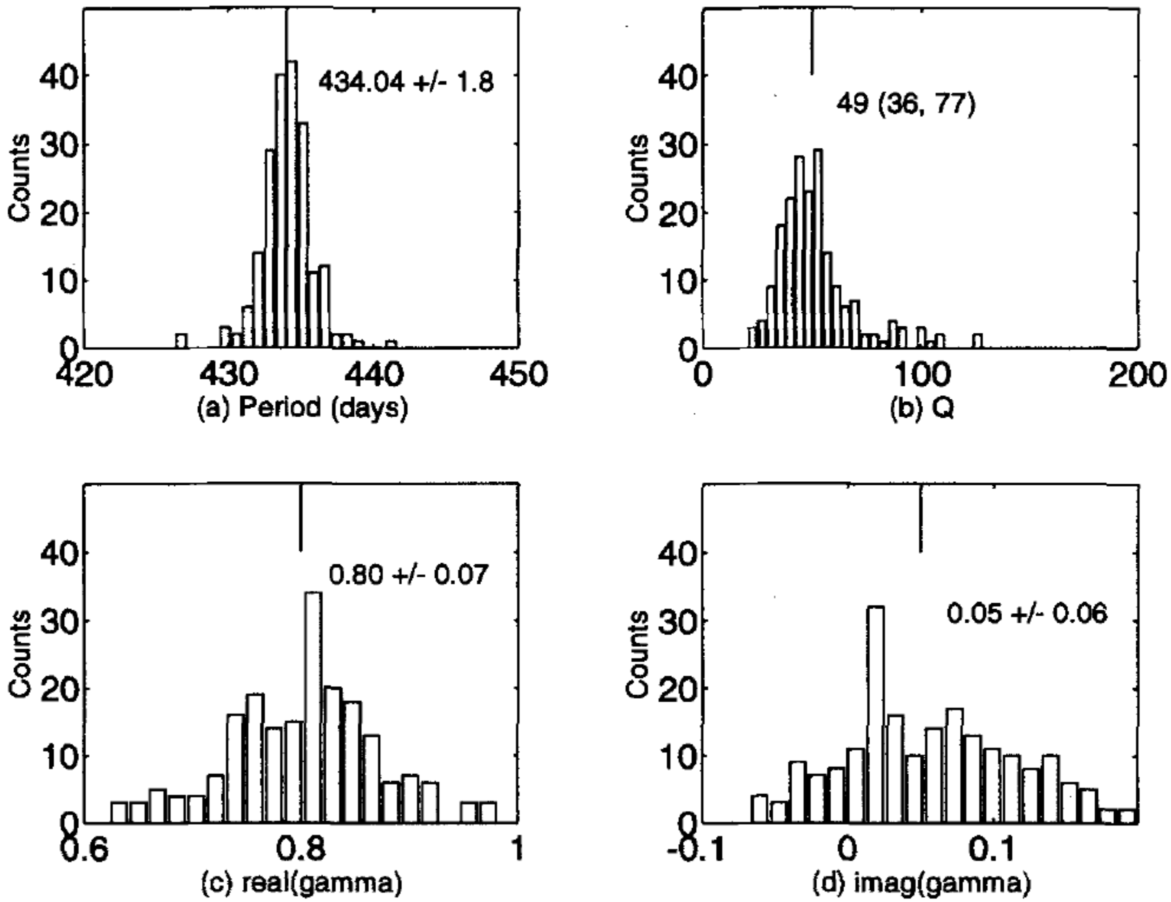

- 200 simulations
- The 'natural' variables that are characterized best by normal distributions.

2

Results Ib.

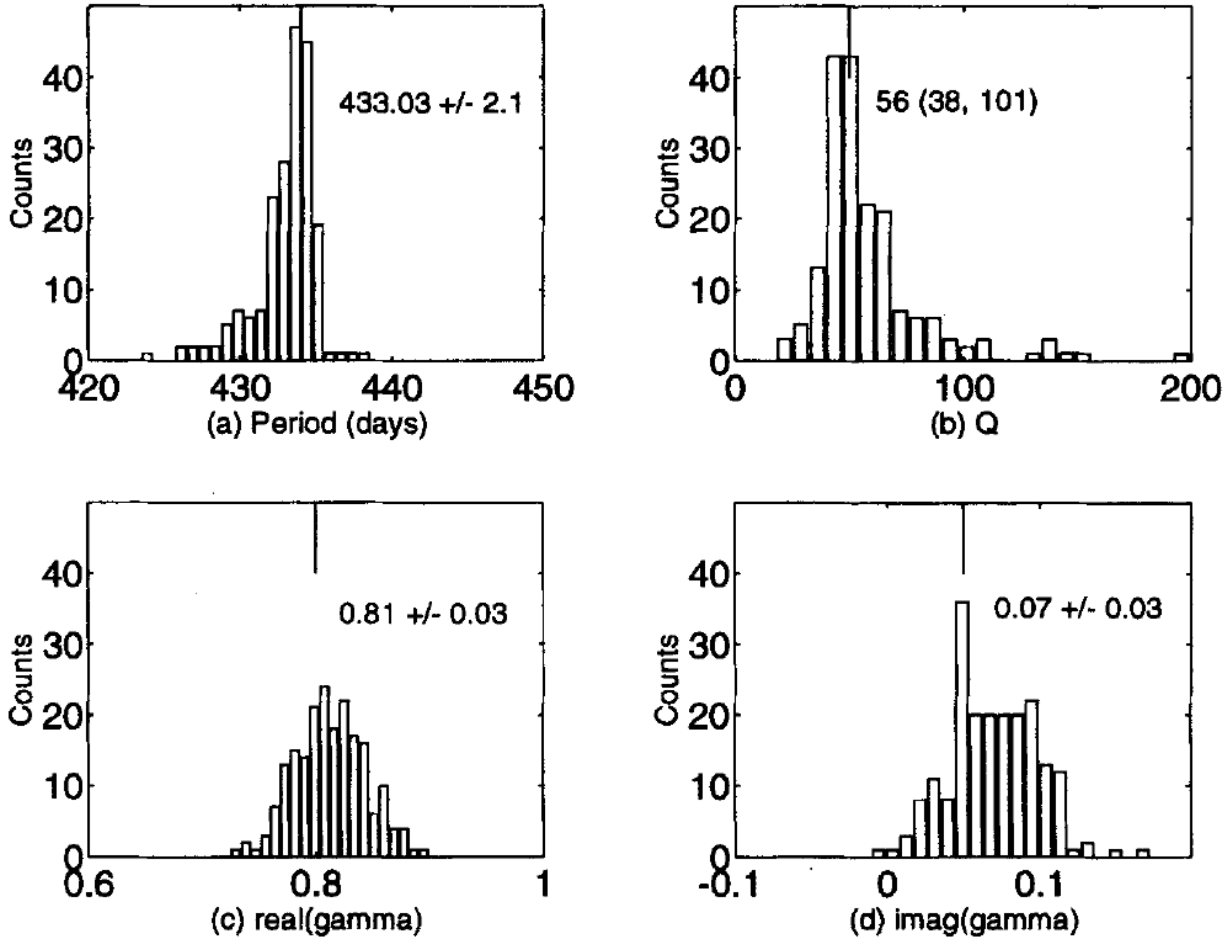
Counts
433.03 +/- 2.1
(a) Period (days)
56 (38, 101)
(b) Q
0.81 +/- 0.03
(c) real(gamma)
0.07 +/- 0.03
(d) imag(gamma)

Results Ic.

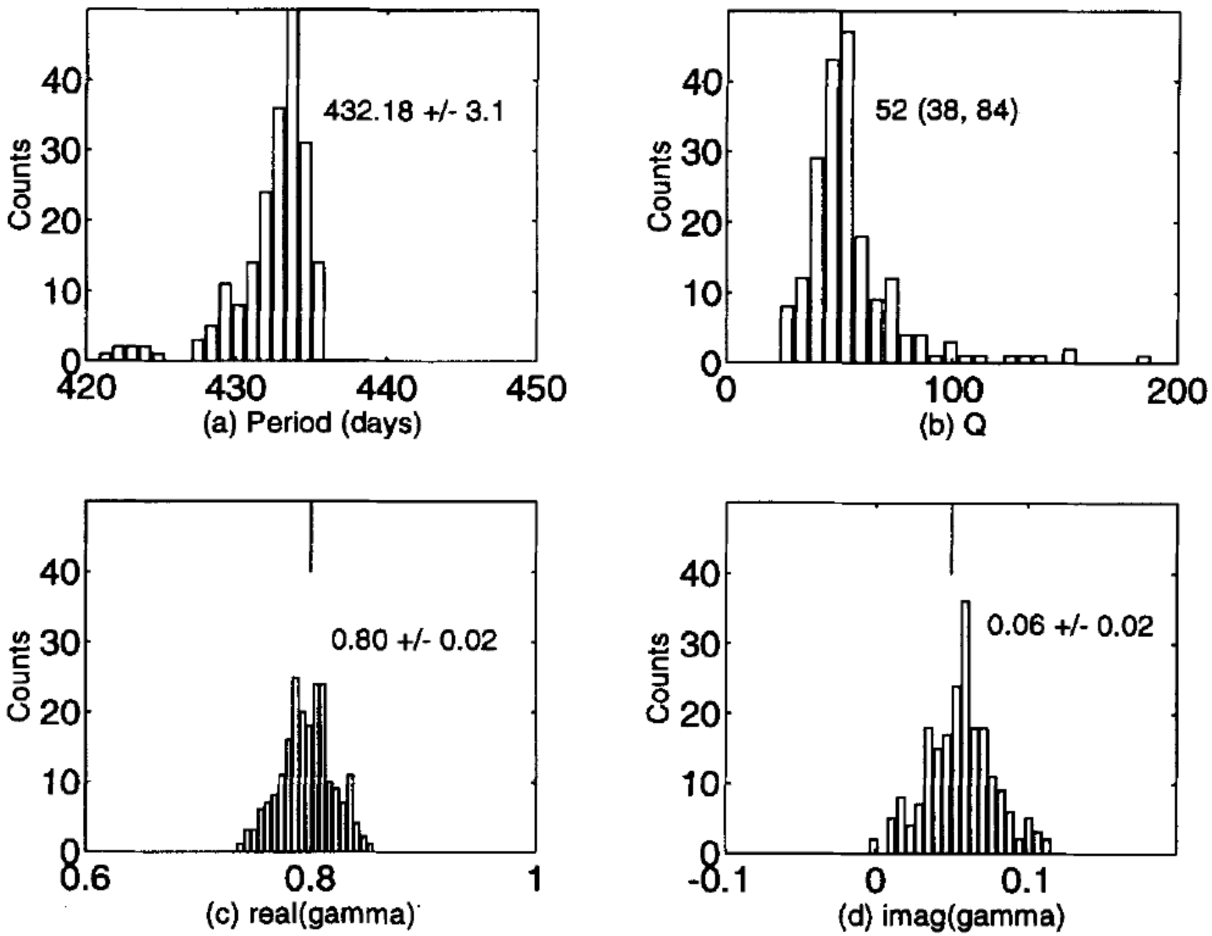

The increasingly more significant skewness and biases with the broader band in which R is minimized confirm the aforementioned biasing effect due to excitations that are not accounted for.

Results II

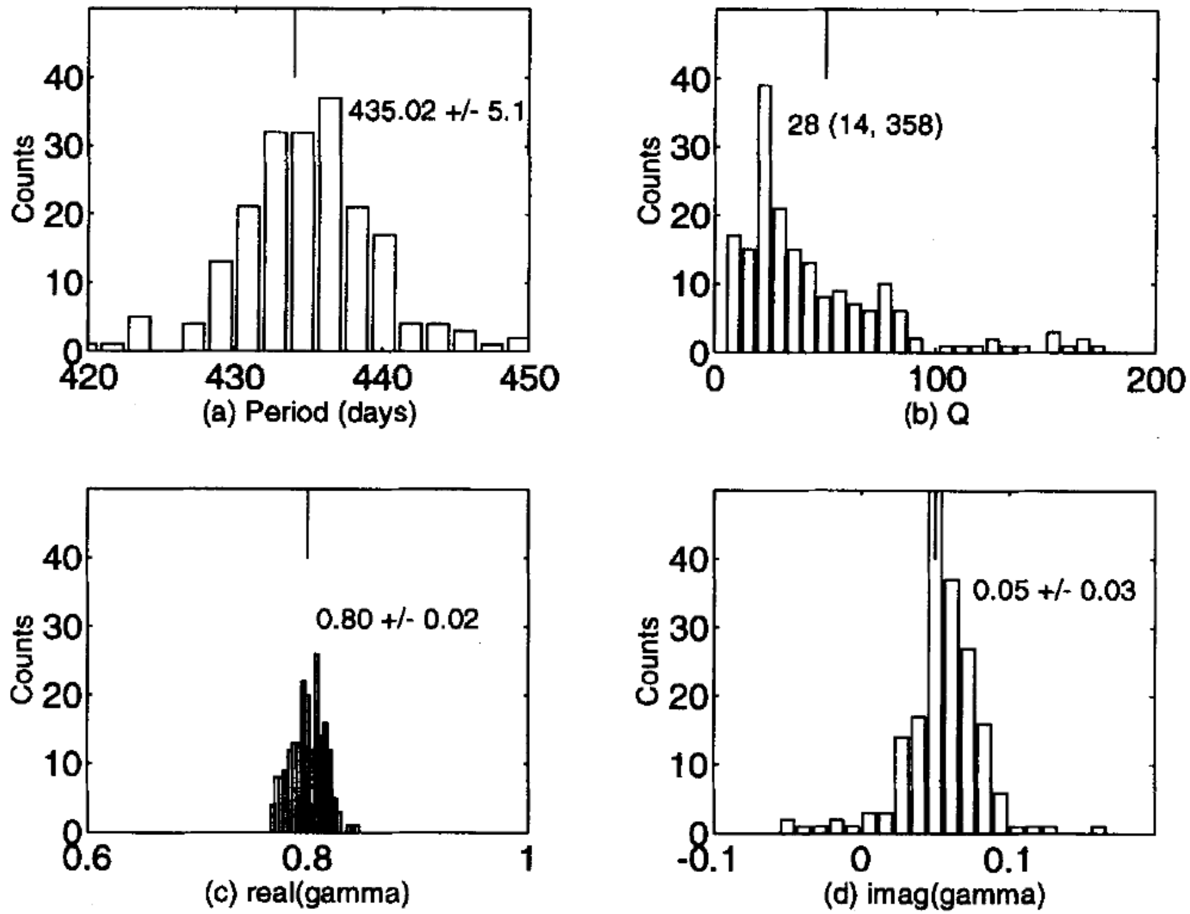

Criterion II yields a distribution that is biased toward low Q values and is poorly constrained *28 (14, 358).*

Results and discussions

Estimator	Period (days)	Q (range)	γ
Criterion Ia (4-bin)	433.7 ± 1.8	49 (36, 77)	$0.84 + 0.073i$
Criterion Ib (64-bin)	431.0 ± 2.1	42 (31, 64)	$0.93 + 0.16i$
Criterion Ic (134-bin)	430.8 ± 3.1	41 (31, 59)	$0.86 + 0.14i$
Criterion II	434.3 ± 5.1	27 (14, 239)	$0.74 + 0.047i$

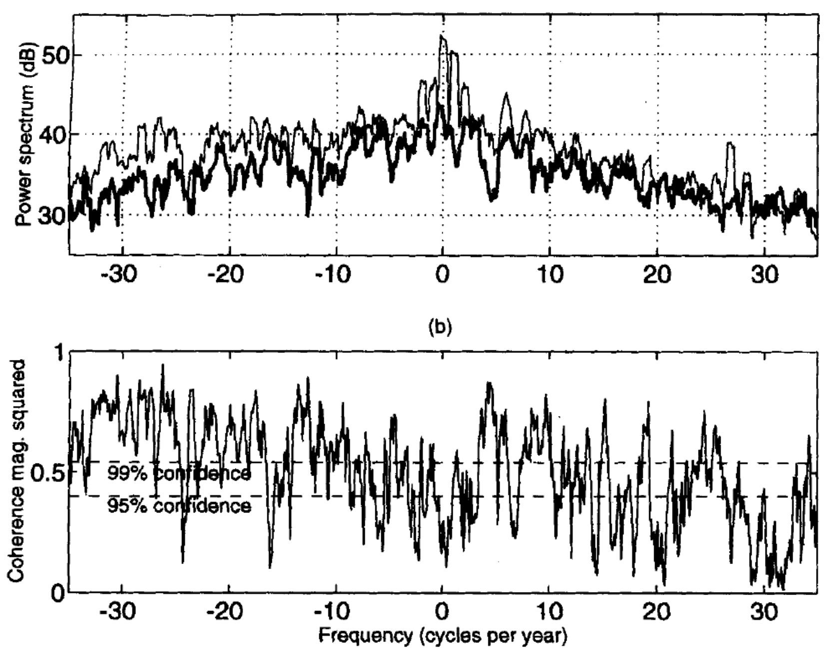

Thick curve ： X_{na}

Thin curve ： X

conclusions

- Our Q estimates are considerably lower than most previous estimates based on ILS data. For time spans comparable to or longer than Q cycles, the excitation is an important factor that maintains the wobble at amplitudes higher than would be the case without the excitation.

Study	Period (days)	*Q* (range)	Data (length in yr)
Jeffreys (1940)	446.7 ± 6.8	46 (37, 60)	ILS (42)
Jeffreys (1968)	433.2 ± 3.4	61 (37, 193)	ILS (68)
Wilson & Haubrich (1976)	434.0 ± 2.5	100 (50, 400)	ILS (70)
Ooe (1978)	434.8 ± 2.0	96 (50, 300)	ILS (76)
Wilson & Vicente (1980)	433.3 ± 3.6	175 (48, 1000)	ILS (78)
Wilson & Vicente (1990)	433.0 ± 1.1	179 (74, 789)	ILS+BIH (86)
Kuehne *et al.* (1996)	439.5 ± 1.2	---	Space93+AAM (9)
This Study	433.7 ± 1.8	49 (35, 100)	Space94+AAM (11)

2

conclusions

- Finally, we note that the y estimates range mostly around 0.7 to 0.9. This means that the overall behavior of the ocean is close to IB, at roughly the 80 per cent level, in polar motion excitation on timescales of months to years.

※inverted barometer (IB)

Data

- International Earth Rotation Service (IERS)
  - IERS C01 (1861.0-1997)
  - IERS C01 (1899.7-1992)
- Re-analysis of the classical astronomical observations using the HIPPARCOS reference frame [Vonrak 1999] [Vonrak 2000]
  - OA97 (1899.7-1992.0)
  - OA99 (1899.7-1992.0)

Linear drift of polar motion

$$x_p = a \cdot t + b + R_{1a}\cos(\varphi_{1a} + \omega_1 t) + R_{2a}\cos(\varphi_{2a} + \omega_2 t)$$
$$y_p = c \cdot t + d + R_{1b}\sin(\varphi_{1b} + \omega_1 t) + R_{2b}\sin(\varphi_{2b} + \omega_2 t)$$

CW : $R_{1a},\ R_{1b},\ \omega_1,\ \varphi_{1a},\ \varphi_{1b}$

AW : $R_{2a},\ R_{2b},\ \omega_2,\ \varphi_{2a},\ \varphi_{2b}$

Weighting function

- Pi=1
- Pi=const/σ_i^2
- Pi=const/(σ_i^2 + σ_0^2)

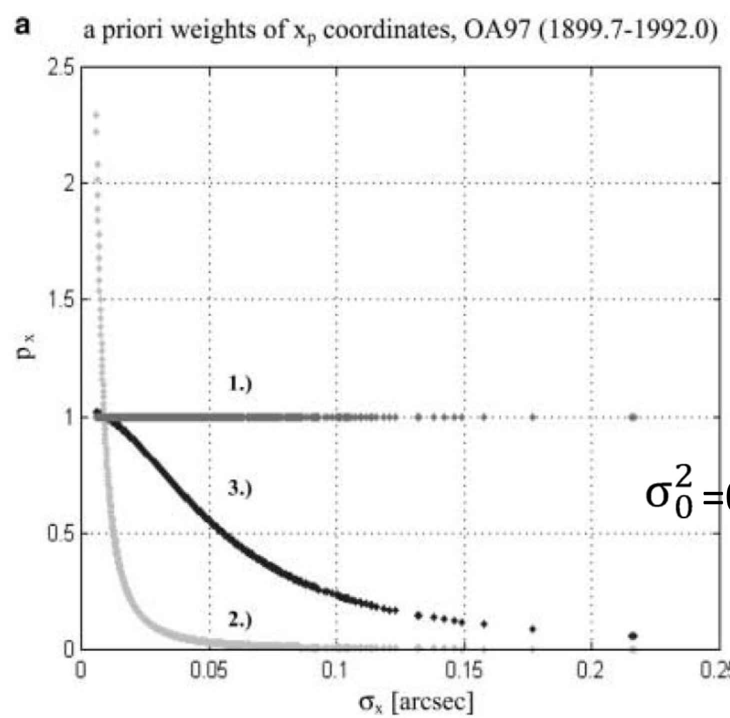

σ_0^2 =0.054

3

	$p_i = 1.0$		$p_i = \frac{\text{const}}{\sigma_i^2}$		$p_i = \frac{\text{const}}{\sigma_i^2+\sigma_0^2}$	
	sec p.m. (mas/year)	dir [deg]	sec p.m. (mas/year)	dir [deg]	sec p.m. (mas/year)	dir [deg]
IERS C01 (1899–1992)	4.38 ± 0.08	77.43 ± 1.06	6.02 ± 0.13	85.16 ± 1.25	4.43 ± 0.08	78.15 ± 1.00
IERS C01 (1861–1997)	3.58 ± 0.05	75.53 ± 0.85	4.49 ± 0.10	82.29 ± 1.24	4.00 ± 0.06	77.36 ± 0.77
OA97 (1899–1992) uncorrelated	3.38 ± 0.05	78.69 ± 0.80	3.80 ± 0.04	82.73 ± 0.65	3.40 ± 0.05	79.27 ± 0.76
OA97 (1899–1992) correlated	3.27 ± 0.05	75.11 ± 0.84	3.78 ± 0.04	80.59 ± 0.65	*3.31 ± 0.05*	*76.08 ± 0.80*
OA99 (1899–1992) uncorrelated	2.85 ± 0.05	73.55 ± 0.93	2.49 ± 0.04	71.54 ± 0.95	2.81 ± 0.04	73.46 ± 0.90
OA99 (1899–1992) correlated	2.85 ± 0.04	75.52 ± 0.90	2.48 ± 0.04	73.04 ± 0.96	2.81 ± 0.04	75.45 ± 0.90

Approach 3. is considered as most satisfactory.

The most plausible result for the linear drift of the pole in the 20th century a drift of 3.31 ± 0.05 ms/yr in the direction of 76.1 ± 0.80 ° west longitude.

CW period: 1.17428 ± 0.00009 years

CW amplitude:

semi-major axis $R_{1a} = 0.1217 \pm 0.0017$ arcseconds

semi-minor axis $R_{1b} = 0.1037 \pm 0.0017$ arcseconds

AW period: 1.00055 ± 0.00008 years

AW amplitude:

semi-major axis $R_{2a} = 0.0992 \pm 0.0017$ arcseconds

semi-minor axis $R_{2b} = 0.0836 \pm 0.0017$ arcseconds.

3

Wavelet Analysis

[Chao and Naito, 1995]

$$W_{\psi}(f)(a,b) = \frac{1}{\sqrt{a}} \int_{-\infty}^{\infty} f(t)\,\psi\left(\frac{t-b}{a}\right) dt$$

$\psi(t)$ basic wavelet

a is the dilation/compression scale factor that determines the characteristic frequency

b is the sliding factor, translation in the time domain

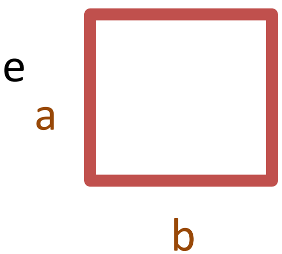

- Morlet wavelet (Morlet et al., 1982)

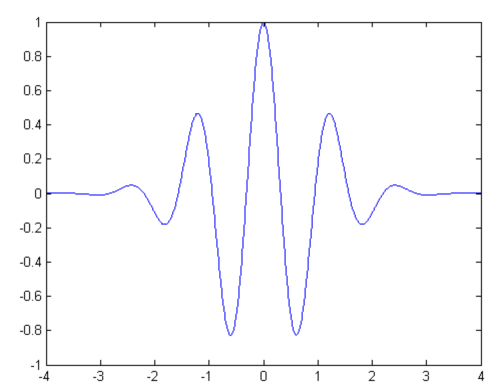

Wavelet spectra

- OA97 (1899.7-1992.0) for AW

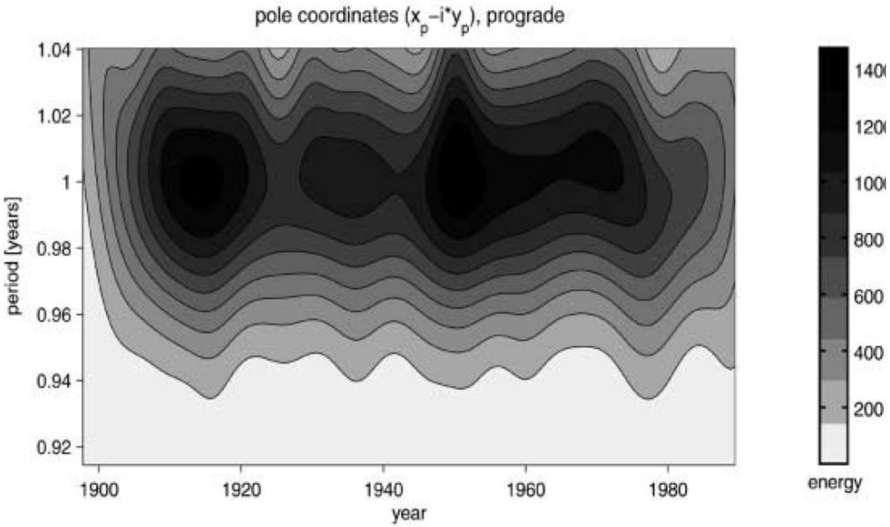

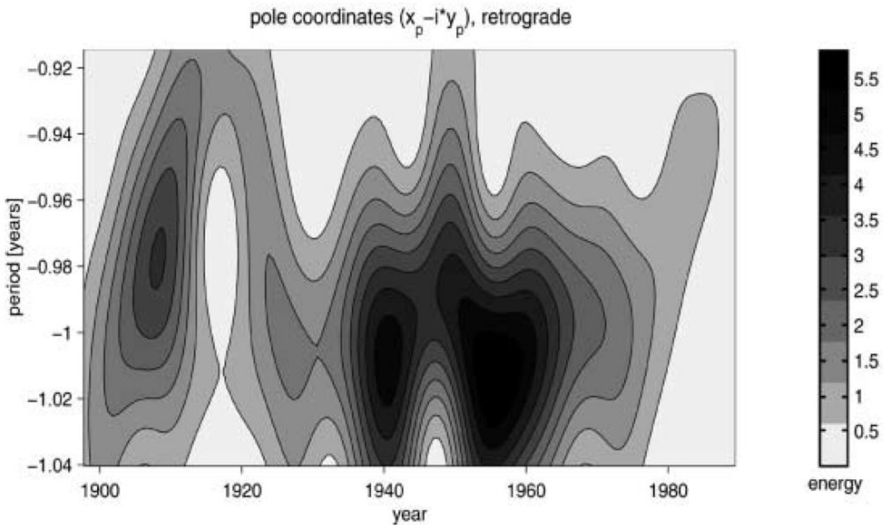

Clear maxima of the weak retro grade AW occurred around 1908, 1940 and 1955.

Sliding window analysis

Window size is set to 13.76 year

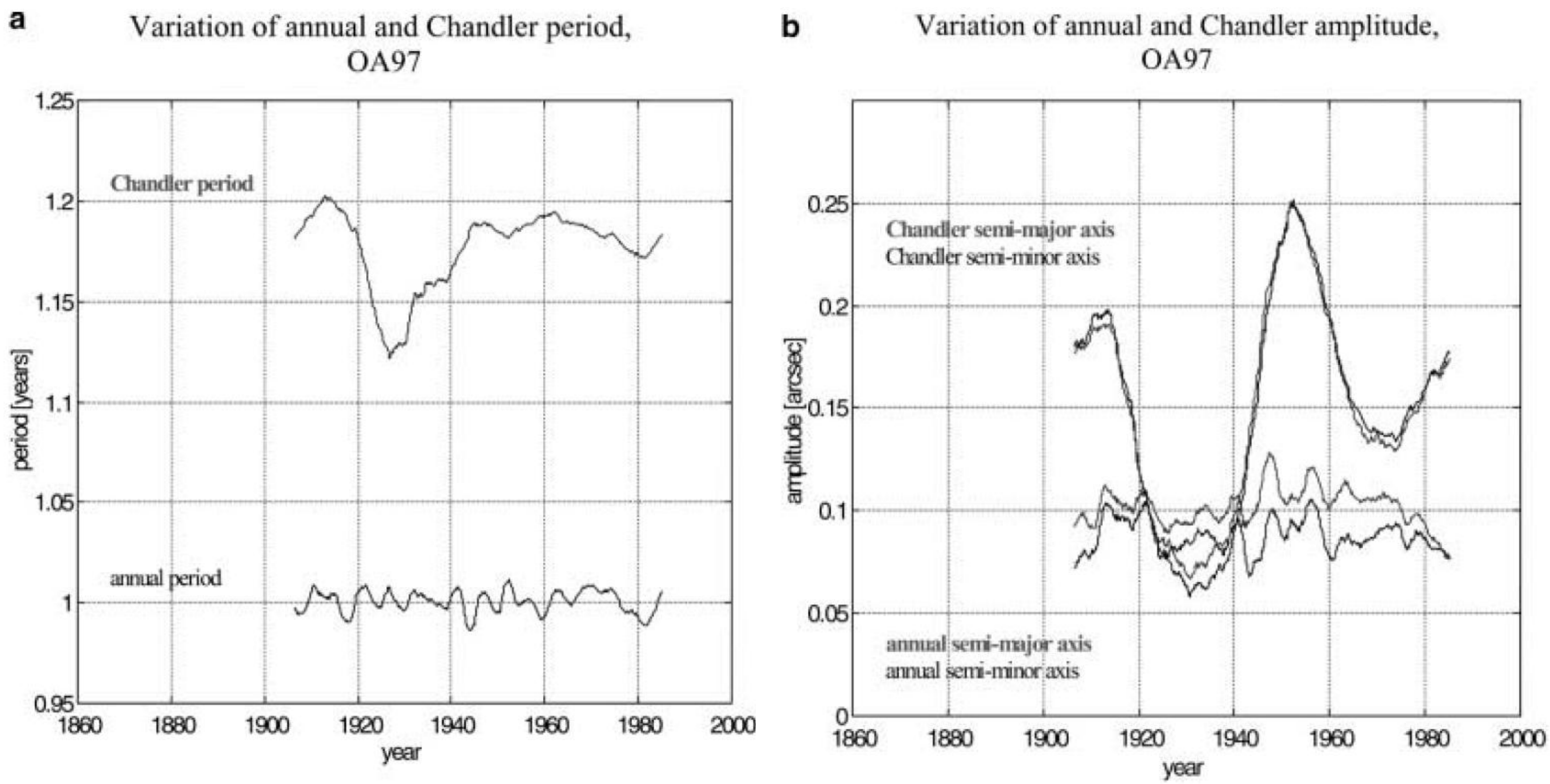

Wavelet analysis of CW parameters

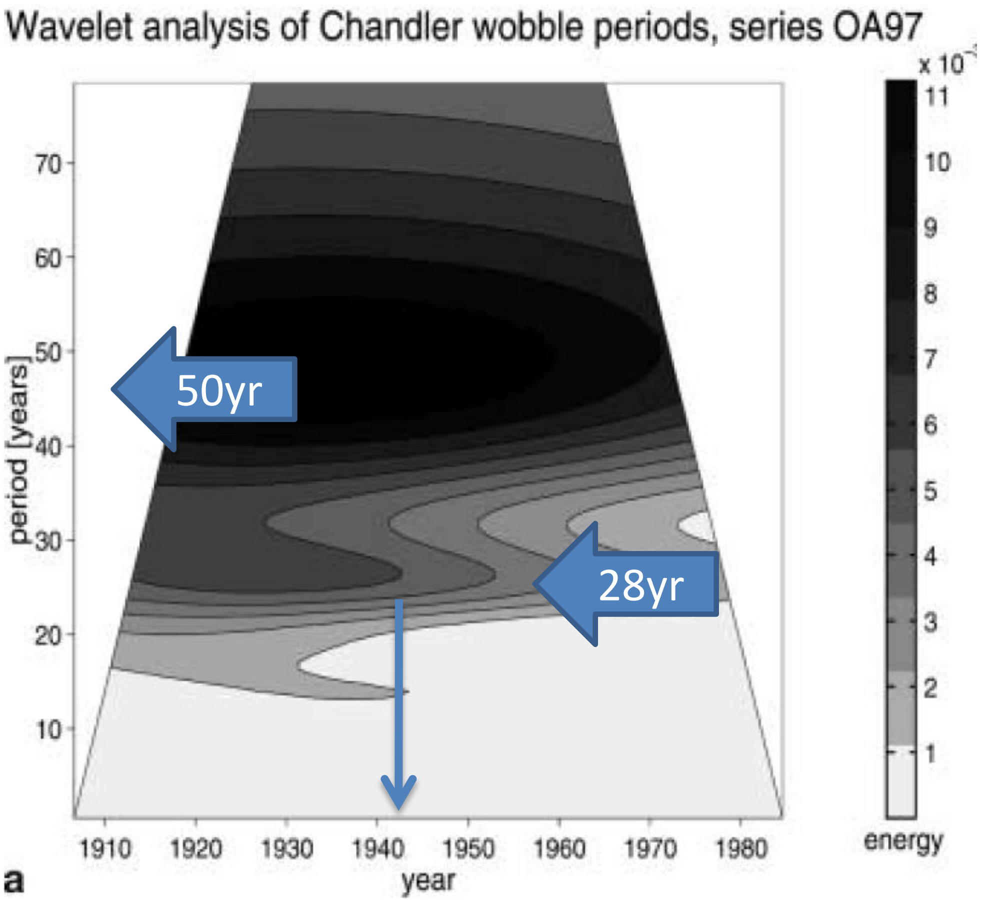

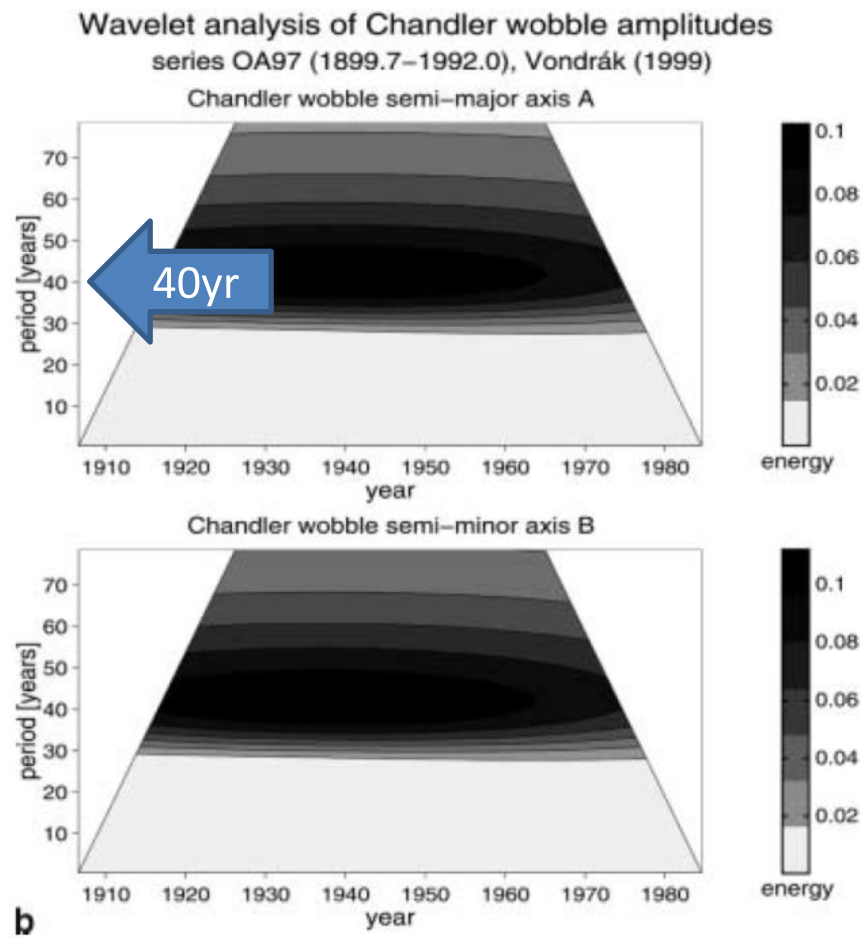

In principle, the main period (40-50 years) of the CW parameters, could be explained by a beat of two oscillations with close period.

Wavelet analysis of AW parameters

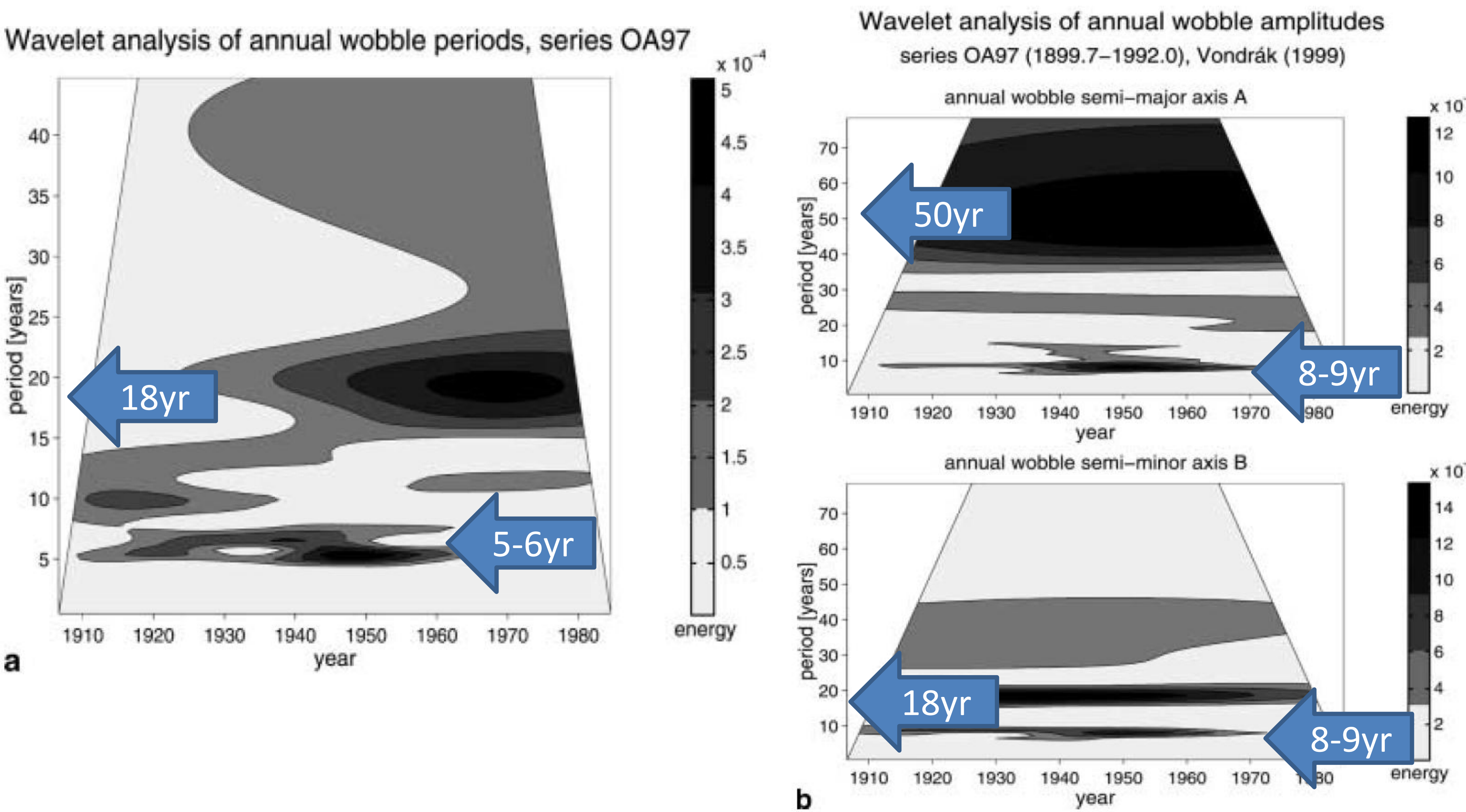

conclusions

- The existence of multiple periods is certainly not a consequence of some spectral splitting phenomenon. The answer, then, presumably lies in the existence of inelastic layers in the earth (hydrosphere, asthenosphere, and outer core) and the coupling thereof with the elastic parts of the earth.
- Q estimates are associated with large uncertainties inevitable in situations where the record length is much shorter than the decay

Thanks for your attentions!